Cylindrical Microstrip Line Partially Embedded in a Perfectly Conducting Ground Plane

Hesham A. Auda

Abstract—**The quasi-TEM characteristics of a novel cylindrical microstrip line are rigorously determined. The line consists of an infinitesimally thin strip on the surface of a dielectric cylinder partially embedded in a perfectly conducting ground plane. Expressions for the potential distribution inside and outside the dielectric substrate, the charge distribution on the strip, and the capacitance of the microstrip line are derived. Sample numerical results based on the derived expressions are also given and discussed. In particular, it is shown that the effective dielectric constant for the symmetrical microstrip line is a linear function of the substrate's dielectric constant, and is almost independent of the strip width.**

I. Introduction

Conformal microstrip lines on cylindrical and elliptic dielectric substrates are widely utilized in the excitation of conformal missile antennas and arrays, and have therefore become the focus of increasingly active research efforts. Much of the previous research has been directed toward determining the quasi-TEM characteristics of cylindrical and elliptic striplines and microstrip lines in homogeneous free space. In this type of analysis, the characteristic impedance and propagation constant of the quasi-TEM mode of the line are determined in terms of the static capacitance of the line. Among the methods used with success are conformal mapping [1]–[3], numerical solution of Laplace's equation in cylindrical and elliptic coordinate systems [4], [5], and spectral-domain [6] and Green's-function-based integral equation [7] techniques.

In this paper, the quasi-TEM characteristics of a novel cylindrical microstrip line are rigorously determined. The line consists of an infinitesimally thin strip on the surface of a dielectric cylinder partially embedded in a perfectly conducting ground plane (see Fig. 1). The microstrip structure is referred to as cylindrical microstrip line because of its cylindrical substrate. The line geometry can be generalized to a configuration which has found wide application in the design of cylindrical radiating structures [8] by placing cylindrical or elliptic substrate on a dented perfectly conducting wedge. In addition, the new microstrip line may be considered a possible alternative to the familiar planar microstrip line. The new line has a distinct advantage over the planar line with regard to the amount of dielectric material saved and the rigor with which coupling between multiple microstrip lines can be studied. It also combines, particularly in the case of wide strips, the coplanar waveguide and conductor-backed coplanar waveguide structures in one structure [9]. The merits of the proposed line revealed here further demonstrate its practical significance.

The method of analysis utilized relies on the derivation of the exact potential distributions outside and inside the dielectric cylinder. The potentials are constructed in such a way that the continuity of the potential and, hence, the continuity of the tangential component of the electric field across the dielectric interface are automatically enforced. Boundary condition equations for the problem are obtained from enforcing the potential to have a specified constant value on the strip and from satisfying the jump discontinuity in the normal derivative of the potential across the dielectric interface. The two equations are subsequently combined and solved using Galerkin's method. Expressions for the charge distribution on the strip and the capacitance of the microstrip line are then obtained. Sample numerical results based on the derived expressions are also given and discussed. In particular, it is shown that the effective dielectric constant for the symmetrical microstrip line is a linear function of the substrate's dielectric constant, and is almost independent of the strip width.

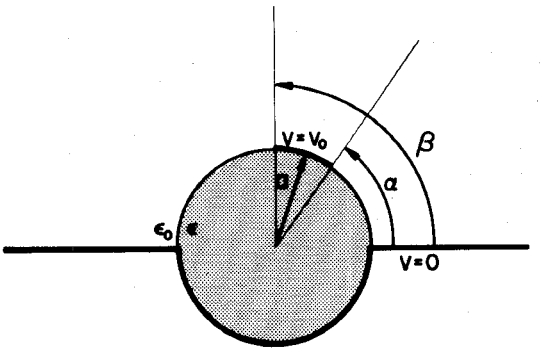

Fig. 1. Cylindrical microstrip line partially embedded in a perfectly conducting ground plane.

II. Formulation

The successful analysis of the partially embedded cylindrical microstrip line hinges on the construction of the exact potentials both outside and inside the dielectric cylinder.

The potential outside the dielectric cylinder is constructed such that it satisfies Laplace's equation $\nabla^2 V_F(\rho,\phi)=0$, $\rho \geqslant a$, $0 \leqslant \phi \leqslant \pi$, subject to the boundary conditions that $V_F(a,\phi)=\Phi(\phi)$, $0 \leqslant \phi \leqslant \pi$, and $V_F(\rho,0)=V_F(\rho,\pi)=0$, for $\rho \geqslant a$. Furthermore, the potential must be both finite and continuous everywhere and regular at infinity. The solution of Laplace's equation in this region can be obtained using the method of separation of variables [10, section 4-2] as

$$V_F(\rho,\phi)=\sum_{n=1}^{\infty} V_n\left(\frac{a}{\rho}\right)^n \sin(n\phi) \tag{1}$$

where

$$V_n=\frac{2}{\pi}\int_0^{\pi}\Phi(\phi)\sin(n\phi)\,d\phi. \tag{2}$$

On the other hand, the potential inside the dielectric cylinder satisfies the Laplace equation $\nabla^2 V_D(\rho,\phi)=0$, $\rho \leqslant a$, $0 \leqslant \phi \leqslant 2\pi$, subject to the boundary conditions that $V_D(a,\phi)=\Phi(\phi)$, $0 \leqslant \phi \leqslant \pi$, and is zero for $\pi \leqslant \phi \leqslant 2\pi$. Furthermore, the potential must be both finite and continuous at all points inside the cylinder and on its boundary. The solution of Laplace's equation in this region can likewise be obtained using the method of

Manuscript received January 10, 1990; revised April 23, 1991. This work was supported in part by the School of Engineering, University of Mississippi, University, MS 38677.

The author was with the Department of Electrical Engineering, University of Mississippi, University, MS 38677. He is now with the Kato Group, 4 Behler Passage, Kasr El Nil Street, Cairo, Egypt.

IEEE Log Number 9101654.

separation of variables as

$$V_D(\rho,\phi)=\sum_{n=1}^{\infty}V_n'\left(\frac{\rho}{a}\right)^n\sin(n\phi)+\sum_{n=0}^{\infty}V_n''\left(\frac{\rho}{a}\right)^n\cos(n\phi) \quad (3)$$

where

$$V_n'=\frac{1}{\pi}\int_0^{\pi}\Phi(\phi)\sin(n\phi)\,d\phi \quad (4)$$

$$V_n''=\frac{\upsilon_n}{2\pi}\int_0^{\pi}\Phi(\phi)\cos(n\phi)\,d\phi \quad (5)$$

and υ_n is the Neumann number (with $\upsilon_0=1$, and $\upsilon_n=2$ for $n\geqslant 1$).

III. Equations of the Problem

The potentials outside and inside the dielectric cylinder have been constructed in the previous section in such a way that their continuity across the dielectric interface and, hence, the continuity of the tangential component of the electric field [11, section 3-2] are automatically enforced. It therefore only remains to satisfy the requirement of constant potential, or zero tangential electric field, at the strip, viz.,

$$\Phi(\phi)=V_0, \qquad \alpha\leqslant\phi\leqslant\beta. \quad (6)$$

Furthermore, the normal component of the displacement vector, $\boldsymbol{D}=\epsilon\boldsymbol{E}=-\epsilon\nabla V$, is discontinuous across the dielectric interface by the amount of the surface free charge density, σ, on the strip. Consequently,

$$\epsilon_r\frac{\partial}{\partial\rho}V_D(a,\phi)-\frac{\partial}{\partial\rho}V_F(a,\phi)=\begin{cases}\dfrac{1}{\epsilon_0}\sigma(\phi), & \alpha\leqslant\phi\leqslant\beta\\ 0, & \text{otherwise.}\end{cases} \quad (7)$$

IV. Galerkin's Solution

Equation (6) and the last line of (7) are sufficient for the complete evaluation of the potential Φ on the dielectric interface. A Galerkin solution of the pair of equations can be attained by expanding Φ in terms of a complete set of orthogonal functions on the dielectric interface. The expansion functions need also be chosen so that $\Phi(0)=\Phi(\pi)=0$. An appropriate expansion of Φ is therefore

$$\Phi(\phi)=V_0\sum_{k=1}^{\infty}a_k\sin(k\phi) \quad (8)$$

where a_k are real coefficients to be determined.

Using the expansion (8), the potentials outside and inside the dielectric cylinder are readily found as

$$V_F(\rho,\phi)=V_0\sum_{n=1}^{\infty}a_n\left(\frac{a}{\rho}\right)^n\sin(n\phi) \quad (9)$$

$$V_D(\rho,\phi)=\frac{1}{2}V_0\sum_{n=1}^{\infty}a_n\left(\frac{\rho}{a}\right)^n\sin(n\phi)+\frac{1}{2\pi}V_0\sum_{k=1}^{\infty}a_k\sum_{n=0}^{\infty}\upsilon_n Sc_{kn}(0,\pi)\left(\frac{\rho}{a}\right)^n\cos(n\phi). \quad (10)$$

In (10),

$$Sc_{kn}=\int\sin(k\phi)\cos(n\phi)\,d\phi=\begin{cases}-\dfrac{1}{4k}\cos(2k\phi), & n=k\neq 0\\ \dfrac{1}{n^2-k^2}\left(k\cos(k\phi)\cos(n\phi)+n\sin(k\phi)\sin(n\phi)\right), & n\neq k\end{cases} \quad (11)$$

where $Sc_{kn}(p,q)$ indicates that the integration in (11) is taken over ϕ from p to q. Substituting (9) and (10) into (6) and the last line of (7), there then results, after some manipulation,

$$\sum_{k=1}^{\infty}a_k\sin(k\phi)=1, \qquad \alpha\leqslant\phi\leqslant\beta \quad (12)$$

$$\sum_{k=1}^{\infty}a_k\left((2+\epsilon_r)k\sin(k\phi)+\frac{2}{\pi}\epsilon_r\sum_{n=1}^{\infty}nSc_{kn}(0,\pi)\cos(n\phi)\right)=0, \qquad 0\leqslant\Phi<\alpha \text{ or } \beta<\phi\leqslant\pi. \quad (13)$$

Testing (12) and (13) with $\sin(m\phi)$, $m=1,2,\cdots$, there finally results the system of algebraic equations

$$\boldsymbol{Xa}=\boldsymbol{b} \quad (14)$$

where $\boldsymbol{a}=[a_k]$ is the vector of the unknown coefficients, and

$$\boldsymbol{X}=[X_{mk}]=\left[Ss_{mk}(\alpha,\beta)+(2+\epsilon_r)k\left(Ss_{mk}(0,\alpha)+Ss_{mk}(\beta,\pi)\right)+\frac{2}{\pi}\epsilon_r\sum_{n=1}^{\infty}nSc_{kn}(0,\pi)\left(Sc_{mn}(0,\alpha)+Sc_{mn}(\beta,\pi)\right)\right] \quad (15)$$

$$\boldsymbol{b}=[b_m]=\left[\frac{1}{m}\left(\cos(m\alpha)-\cos(m\beta)\right)\right]. \quad (16)$$

In (15),

$$Ss_{mk}=\int\sin(m\phi)\sin(k\phi)\,d\phi=\begin{cases}\dfrac{1}{2}\phi-\dfrac{1}{4k}\sin(2k\phi), & m=k\neq 0\\ \dfrac{1}{m^2-k^2}\left(k\sin(m\phi)\cos(k\phi)-m\cos(m\phi)\sin(k\phi)\right), & m\neq k\end{cases} \quad (17)$$

where $Ss_{mk}(p,q)$ indicates that the integration in (17) is taken over the interval $[p,q]$.

The solution of the system of equations (14) determines the expansion coefficients a_k, $k=1,2,\cdots$, and, hence, the complete potential distribution outside and inside the dielectric cylinder.

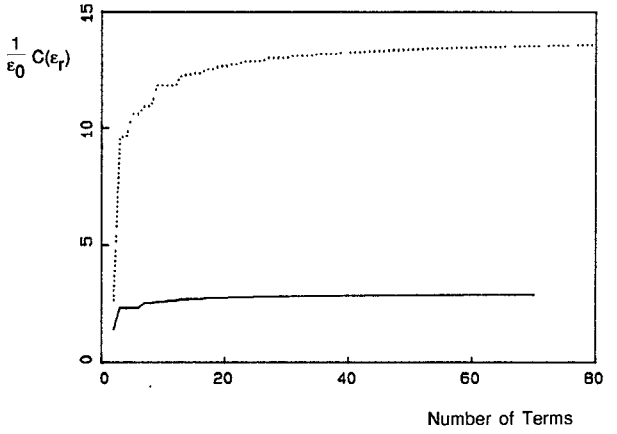

Fig. 2. Convergence of the capacitance of a symmetrical microstrip line: $\alpha = 45°$ and $\beta = 135°$. $\epsilon_r = 1$ (———); $\epsilon_r = 12$ (· · · · ·).

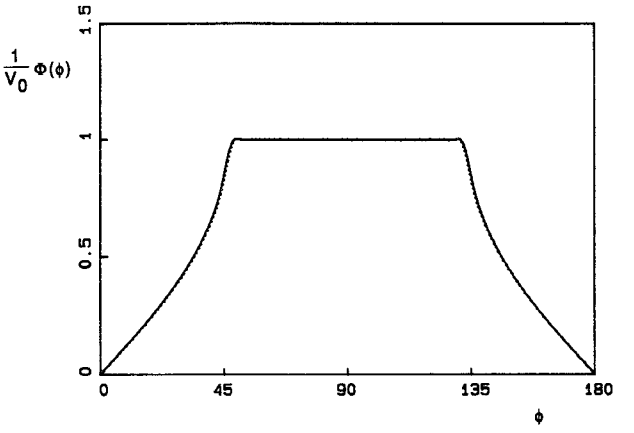

Fig. 3. Potential distribution on the dielectric interface of a symmetrical microstrip line: $\alpha = 45°$ and $\beta = 135°$. $\epsilon_r = 1$ (———); $\epsilon_r = 12$ (· · · · ·).

V. Charge Distribution on the Strip and the Capacitance of the Microstrip Line

Substituting now the fully determined potentials, V_F and V_D, into the first line of (7), the surface free charge density on the strip is readily found as

$$\sigma(\phi) = \frac{1}{2a}\epsilon_0 V_0 \sum_{k=1}^{\infty} a_k \left((2+\epsilon_r) k \sin(k\phi) + \frac{2}{\pi}\epsilon_r \sum_{n=1}^{\infty} n Sc_{kn}(0,\pi)\cos(n\phi) \right), \qquad \alpha \leqslant \phi \leqslant \beta. \quad (18)$$

Consequently, the total charge induced on the strip is given by

$$Q = a\int_{\alpha}^{\beta} \sigma(\phi)\, d\phi = \frac{1}{2}\epsilon_0 V_0 \sum_{k=1}^{\infty} a_k \left((2+\epsilon_r)(\cos(k\alpha) - \cos(k\beta)) + \frac{2}{\pi}\epsilon_r \sum_{n=1}^{\infty} Sc_{kn}(0,\pi)(\sin(n\beta) - \sin(n\alpha)) \right). \quad (19)$$

The capacitance of the microstrip line is then evaluated as $C = Q/V_0$. Since all of the entries in the Galerkin system of equations are independent of the diameter of the dielectric substrate, this will also be true of the capacitance of the line.

VI. Numerical Results and Discussion

The analysis in this paper has been implemented in a FORTRAN program. The potential distribution on the dielectric interface, the charge distribution on the strip, and the capacitance of the microstrip line have been computed for a wide variety of parameter values. Sample numerical results are presented in this section.

The convergence of the capacitance of the microstrip line is shown in Fig. 2. The convergence curves obtained pertain to a wide symmetrical strip ($\alpha = 45°$ and $\beta = 135°$) on the interface of a dielectrical cylinder with dielectric constants $\epsilon_r = 1$ and $\epsilon_r = 12$. Two remarks can be made on the figure. First, a relatively large number of expansion functions are needed for the convergence of the solution. However, because all of the series in the expressions for the matrix elements and the capacitance are rapidly convergent, the run time is exceptionally fast. Second, the convergence curves exhibit a stairlike behavior, which can be explained in view of the symmetry of the strip about $\phi = 90°$ and the symmetry and asymmetry properties of the cosine function in the elements of the right-hand-side vector. Similar convergence characteristics have been observed in the case of a narrow symmetrical strip ($\alpha = 85°$ and $\beta = 95°$) as well.

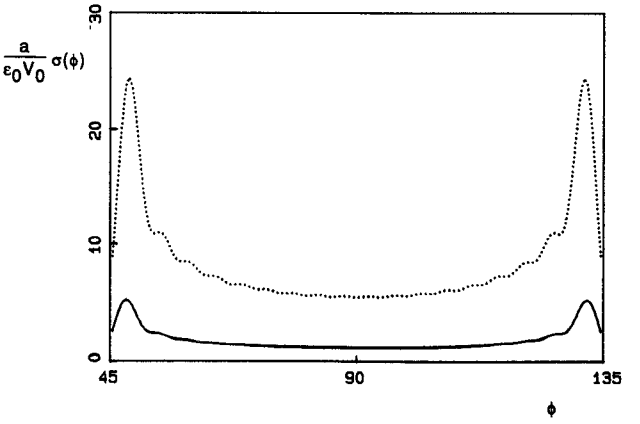

Fig. 4. Charge distribution on the strip of a symmetrical microstrip line: $\alpha = 45°$ and $\beta = 135°$. $\epsilon_r = 1$ (———); $\epsilon_r = 12$ (· · · · ·).

The corresponding normalized potential and charge distributions on the dielectric interface and strip are shown in Figs. 3 and 4, respectively. As can be seen from Fig. 3, the normalized potential attains the boundary value of unity with high precision. Furthermore, the potential is quite insensitive to the value of the dielectric constant. In contrast, an examination of Fig. 4 shows that the effect of the dielectric constant on the charge distribution is pronounced. Another characteristic of the charge distribution is worth noting. The edge condition requires the limit of the charge distribution as ϕ approaches α or β to be infinity [12]. On the other hand, an entire domain type of expansion has been utilized to represent a charge distribution that identically vanishes outside the strip. The combined effect of these two situations is readily seen in the forced descent of the charge distribution as it approaches the two edges so as to obtain the average of the two side limits at each edge, as demanded by the theory of Fourier series. The oscillations in the charge distribution associated with the Gibbs phenomenon have substantially been reduced by utilizing the Lanczos conver-

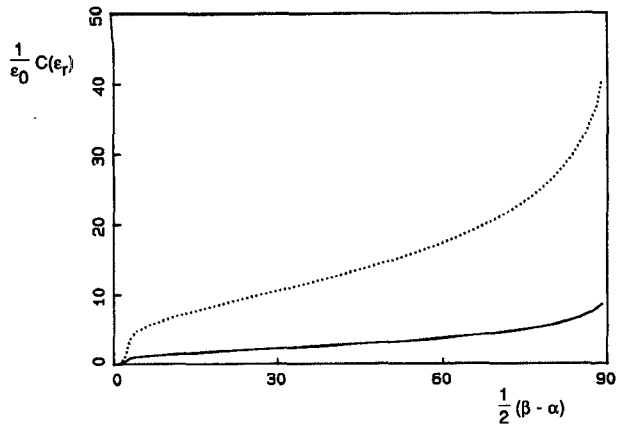

Fig. 5. Change of the capacitance of a symmetrical microstrip line with the strip width: $\alpha = 45°$ and $\beta = 135°$. $\epsilon_r = 1$ (———); $\epsilon_r = 12$ (· · · · ·).

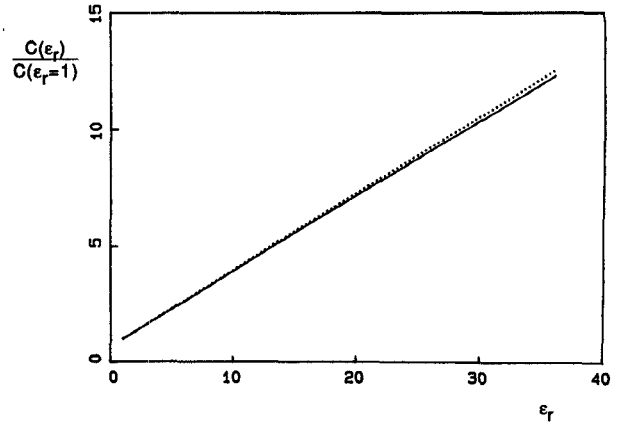

Fig. 6. Change of the normalized capacitance $C(\epsilon_r) \div C(\epsilon_r = 1)$ (the effective dielectric constant) of a symmetrical microstrip line with the dielectric constant for $\alpha = 85°$ and $\beta = 95°$ (———) and for $\alpha = 45°$ and $\beta = 135°$ (· · · · ·).

gence factor in the summation of the Fourier series for the charge [13, sections 14-4, 5].

The change of the capacitance of a symmetrical microstrip line with the strip width is shown in Fig. 5. The limiting case of two infinitesimal gaps between the strip and the conducting plane is a standard electrostatic boundary value problem. The solution of the latter problem can be extracted from the analysis presented by setting $\alpha = 0$ and $\beta = \pi$. In this case, the $\cos(n\phi)$ term drops off the potential distribution inside the dielectric cylinder, and the Galerkin matrix reduces to a diagonal matrix ($X_{mk} = 0.5\pi\delta_{mk}$, where δ is the Kronecker delta function). The coefficients of expansion are then readily solved for as

$$a_k + \frac{4}{\pi k}, \qquad k = 1, 3, \cdots. \tag{20}$$

Substituting (20) into (18), the charge distribution density becomes

$$\sigma(\phi) = 2\frac{\epsilon_0 V_0}{\pi a}(2+\epsilon_r) \sum_{k=\text{odd}} \sin(k\phi) = \frac{\epsilon_0 V_0}{\pi a}(2+\epsilon_r)\csc(\phi). \tag{21}$$

Integrating (21) over ϕ from Δ to $\pi - \Delta$, where Δ is the gap width, and dividing the result by V_0, the limiting capacitance is found:

$$C = \frac{2}{\pi}\epsilon_0(2+\epsilon_r)\log\left(\cot\left(\frac{1}{2}\Delta\right)\right) \tag{22}$$

where "log" denotes the natural logarithm. Using (22), the normalized capacitance, C/ϵ_0, for gaps of width $\Delta = 1°$ is 9.055 for $\epsilon_r = 1$ and is 42.258 for $\epsilon_r = 12$, compared, respectively, with 8.589 and 40.692, as obtained from Fig. 2.

Finally, the capacitance of the microstrip line normalized with respect to the capacitance for $\epsilon_r = 1$ is plotted in Fig. 6 for both narrow and wide strips in the dielectric constant range $1 \leqslant \epsilon_r \leqslant 36$. As can be seen, the strip width has an almost negligible effect on the ratio of capacitances. Furthermore, in the dielectric constant range considered, this ratio is a linear function of the dielectric constant. This is quite significant since the ratio $C(\epsilon_r)/C(\epsilon_r = 1)$ is equal to the effective dielectric constant for the microstrip line [14, section II-A]. A simple formula for the effective dielectric constant for the microstrip line is therefore readily found as

$$\epsilon_r^* = \frac{C(\epsilon_r)}{C(\epsilon_r = 1)} = 0.33\epsilon_r + 0.67, \qquad 1 \leqslant \epsilon_r \leqslant 36. \tag{23}$$

In quasi-TEM analysis, the propagation constant, κ, and the characteristic impedance, ζ, of the microstrip line normalized with respect to the values of the corresponding homogeneous ($\epsilon_r = 1$) line, κ_0 and ζ_0, are equal to the square root of the effective dielectric constant and its inverse, respectively. The sensitivities of the normalized propagation constant and the characteristic impedance of the microstrip line with respect to the substrate's dielectric constant are of interest as well. By definition [15, section 9-1], the sensitivity of "A" with respect to "B" is given by

$$S_B^A = \frac{B}{A}\frac{\partial A}{\partial B} = \frac{\partial \log(A)}{\partial \log(B)} \tag{24}$$

whence

$$S_{\epsilon_r}^{\kappa - \kappa_0} = -S_{\epsilon_r}^{\zeta - \zeta_0} = \frac{1}{2}S_{\epsilon_r}^{\epsilon_r^*} = \frac{1}{2}\frac{0.33\epsilon_r}{0.33\epsilon_r + 0.67}, \qquad 1 \leqslant \epsilon_r \leqslant 36 \tag{25}$$

upon using (23). Thus, the sensitivity of the normalized propagation constant (characteristic impedance) of the microstrip line is a bounded ($0.165 \leqslant |S| \leqslant 0.473$ for $1 \leqslant \epsilon_r \leqslant 36$), monotonically increasing (decreasing) function of the substrate's dielectric constant.

VII. Summary

The quasi-TEM characteristics of a novel cylindrical microstrip line have been rigorously determined. The line consists of an infinitesimally thin strip on the surface of a dielectric cylinder partially embedded in a perfectly conducting ground plane. Expressions for the potential distribution inside and outside the dielectric substrate, the charge distribution on the strip, and the capacitance of the microstrip line have been derived. Sample numerical results based on the derived expressions have also been given and discussed. In particular, it has been shown that the effective dielectric constant for the symmetrical microstrip line is a linear function of the substrate's dielectric constant, and is almost independent of the strip width.

References

[1] L.-R. Zeng, "A method of solving complicated boundary value problems with its applications to coupled rods," *Scientia Sinica*, series A, vol. 25, pp. 1099–1133, Oct. 1982.

[2] L.-R. Zeng and Y. Wang, "Accurate solutions of elliptical and cylindrical striplines and microstrip lines," *IEEE Trans. Microwave Theory Tech.*, vol. MTT-34, pp. 259–265, Feb. 1986.

[3] D. Homentcovschi, "A cylindrical multiconductor stripline-like microstrip transmission line," *IEEE Trans. Microwave Theory Tech.*, vol. 37, pp. 497–503, Mar. 1989.

[4] Y.-C. Wang, "Cylindrical and cylindrically wrapped strip and microstrip lines," *IEEE Trans. Microwave Theory Tech.*, vol. MTT-26, pp. 20–23, Jan. 1978.

[5] K. K. Joshi and B. N. Das, "Analysis of elliptic and cylindrical striplines using Laplace's equation," *IEEE Trans. Microwave Theory Tech.*, vol. MTT-28, pp. 381–386, Apr. 1980.

[6] C. H. Chan and R. Mittra, "Analysis of a class of cylindrical multiconductor transmission lines using an iterative approach," *IEEE Trans. Microwave Theory Tech.*, vol. MTT-35, pp. 415–424, Apr. 1987.

[7] N. G. Alexopoulos and A. Nakatani, "Cylindrical substrate microstrip line characterization," *IEEE Trans. Microwave Theory Tech.*, vol. MTT-35, pp. 843–849, Sept. 1987.

[8] J. R. Wait, *Electromagnetic Radiation from Cylindrical Structures*. Elmsford, NY: Pergamon Press, 1959.

[9] T. Itoh, "Overview of quasi-planar transmission lines," *IEEE Trans. Microwave Theory Tech.*, vol. 37, pp. 275–280, Feb. 1989.

[10] R. Plonsey and R. E. Collin, *Principles and Applications of Electromagnetic Fields*. New York: McGraw Hill, 1961.

[11] J. A. Stratton, *Electromagnetic Theory*. New York: McGraw-Hill, 1941.

[12] G. M. L. Gladwell and S. Coen, "A Chebyshev approximation method for microstrip problems," *IEEE Trans. Microwave Theory Tech.*, vol. MTT-23, pp. 865–870, Nov. 1975.

[13] G. Arfken, *Mathematical Methods for Physicists*. New York: Academic Press, 1966.

[14] R. Mittra and T. Itoh, "Analysis of microstrip transmission lines," in *Advances in Microwaves*, L. Young and H. Sobol, Eds. New York: Academic Press, 1974, vol. 8, pp. 67–141.

[15] M. E. Van Valkenburg, *Analog Filter Design*. New York: Holt, Rinehart, and Winston, 1982.

First-Order Model of Symmetrical Six-Port Microstrip Ring Coupler

S. P. Yeo and C. L. Lau

Abstract—**This paper describes, in brief, how the simple eigenmode approach can be utilized to develop a first-order model that yields explicit ready-to-use formulas for predicting the performance characteristics of a symmetrical six-port microstrip ring coupler. Prototype tests conducted over the 2–5 GHz frequency range show the agreement between the predicted and measured values of the coupler's scattering coefficients to be within ± 0.05 for magnitude and $\pm 10°$ for phase.**

I. Introduction

The symmetrical six-port junction (Fig. 1) has over the past few years been attracting the attention of various researchers. Riblet *et al.* [1] designed one for use as a five-way equal power divider, while Judah *et al.* [2] and Yeo *et al.* [3] showed how it could also be utilized in a six-port reflectometer setup.

Manuscript received August 21, 1990; revised April 12, 1991. This work was supported by the Singapore Science Council under Grant RDAS C/81/09.

The authors are with the Electrical Engineering Department, National University of Singapore, 10 Kent Ridge Crescent, Singapore 0511.

IEEE Log Number 9101652.

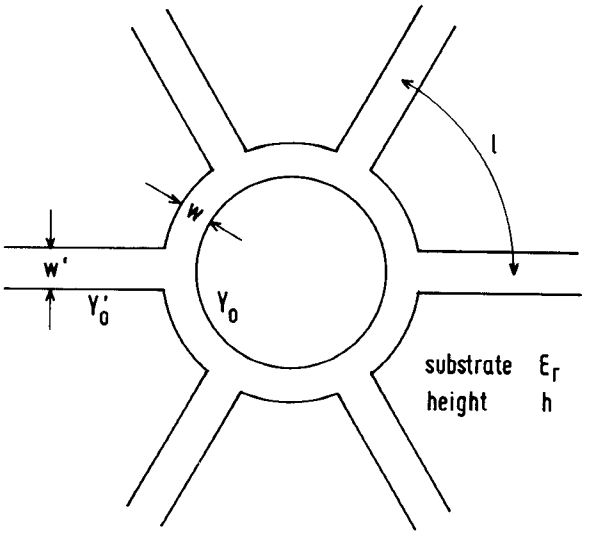

Fig. 1. Symmetrical six-port microstrip ring coupler.

Thus far, satisfactory models to predict the characteristics of the stripline [1] and waveguide [4] versions of the symmetrical six-port junction have been reported in the literature. Our objective in this paper, therefore, is to extend the investigation to include the analysis of the microstrip version. Actually, a model of one such microstrip coupler has already been put forward by Judah *et al.* [2]; however, their circuit topology is more complicated than that of Fig. 1 because they inserted an additional node at the hub of the structure (thereby rendering it, for purposes of analysis, effectively a seven-port instead of a six-port). In contrast, we chose to retain the original simplicity of the ring layout in Fig. 1 so as to obviate the necessity of performing a seven-port to six-port circuit reduction (as Judah *et al.* [2] had to do).

II. Theory

There are two approaches that we can take in the formulation of our model: eigenmode or noneigenmode. The latter has the problem of yielding rather long and unwieldy expressions, although, as one referee has pointed out, it does offer flexibility for studying nonsymmetries in the circuit. The method used in this paper is based on the eigenmode approach since this, as has been demonstrated in previous analyses of the symmetrical N-port junctions [4]–[6], yields simple explicit formulas that can be readily used for design work.

Assuming that the curvature of the central ring line can be ignored (as Cullen *et al.* [7] and Judah *et al.* [2] did in their analyses), we are able to represent the circuit connections between any three consecutive ports $k-1, k, k+1$ by the equivalent transmission-line model of Fig. 2, where, for the mth eigenmode,

$$v_k = v_{k-1} \exp\left(-j\frac{m\pi}{3}\right) = v_{k+1} \exp\left(j\frac{m\pi}{3}\right). \quad (1)$$

0018-9480/91/0900-1666$01.00 ©1991 IEEE